theoretical results in Table 2. These comparisons serve to provide confidence in the validity of the solution. The results obtained using the method presented in this paper are almost identical to the results obtained by Smith.[3] The results shown in Table 2 for the approximate solution were obtained by imposing, on Eq. (2), the condition that $(\lambda_i/m)^2 \ll 1$. The exact solutions are shown to be superior to the approximate solutions, especially for those modes having a small number of circumferential waves. Frequencies, for the first four radial modes having one to five circumferential waves, of a particular shell, subjected to the eight sets of boundary conditions of Table 1, are presented in Table 3.

The advantages of the "exact" solution presented here over those seen previously are: 1) the arbitrary complex constants in the assumed solution need not be redefined as real constants, and 2) the form of the roots of the auxiliary equation need not be monitored during the solution. These advantages yield a saving of computational time and lead to a more truly "general" solution.

### References


[1] Flugge, W., *Stresses in Shells*, Springer-Verlag, Berlin, 1967.

[2] Yu, Y. Y., "Free Vibration of Thin Cylindrical Shells Having Finite Lengths with Freely Supported and Clamped Edges," *Journal of Applied Mechanics*, Vol. 77, 1955, pp. 547–552.

[3] Smith, B. L., "Natural Frequencies of Clamped Cylindrical Shells," *AIAA Journal*, Vol. 6, No. 4, April 1968, pp. 720–721.

[4] Forsberg, K., "Influence of Boundary Conditions on the Modal Characteristics of Thin Cylindrical Shells," *AIAA Journal*, Vol. 2, No. 12, Dec. 1964, pp. 2150–2157.

[5] Koval, L. R. and Cranch, E. T., "On the Free Vibrations of Thin Cylindrical Shells Subjected to an Initial Torque," *Proceedings of the U.S. National Congress of Applied Mechanics*, 1962, pp. 107–117.

[6] Arnold, R. N. and Warburton, G. B., "The Flexural Vibrations of Thin Cylinders," *Proceedings of the Institution of Mechanical Engineers*, Vol. 167, 1951–1953, pp. 62–80.


# Empirical Analysis of Regional Growth Functions of Turbulent Wakes


Andrew H. Jenkins* and Stanley L. Pruett†

*U. S. Army Missile Command, Redstone Arsenal, Ala.*


### Nomenclature

$A_1,A_2$ = regression constants
$B_1,B_2$ = regression coefficients
$d$ = body diameter
$M$ = Mach number
$n$ = number of data points
$N$ = exponent in wake diffusion equations
$P$ = pressure
$r$ = correlation coefficient
$Re$ = Reynolds' number
$x,y$ = physical coordinates
$X$ = $x/d$
$Y$ = $y/d$
$\alpha$ = angle of attack

***Subscripts***

$i$ = $i$th value of $n$ values
$w$ = wake conditions
$\infty$ = freestream conditions

Received April 7, 1969; revision October 20, 1969. Supported under DA Project 1P222901A201.

* Research Aerospace Engineer.

† Aerospace Engineer.

### Introduction

The rate of growth of turbulent viscous wakes of axisymmetric bodies at hypersonic velocities has been of interest for some time. Many investigators[1–6] have developed empirical equations describing the growth as a function of distance behind the body. An empirical relationship of the form $Y = A + BX^N$ has been developed where $N$ has a range of values between 0.25 and 0.67. Most of the experimental investigations covered the far wake region ($X > 150$) at hypersonic Mach numbers ($M_\infty > 6$). Also, a theoretical relationship of the form $Y = (A + BX)^N$ with $N \approx 0.33$ has been derived.[7] Assuming the theoretical model is unbounded as a function of velocity and distance behind the body, then experimental evidence at short distances ($X < 25$) behind the body and at lower Mach numbers ($M_\infty < 6$) is not available for comparison with the theoretical model, except for the evidence of Knystautas.[6]

Experimental data in the distance and Mach number regions of $X < 15$ and $M_\infty < 5$ were analyzed for comparison with the theoretical and experimental models. The experimental data were obtained on the U.S. Army Missile Command's aeroballistic range.

The models used were hemisphere cylinders with a base diameter of 0.226 in. and 1.5 calibers in length. The velocities were $M_\infty \approx 4.2$ and $Re \approx 5.38 \times 10^5$. The wake cores were in all cases turbulent up to the throat.

### Data Analysis

The interface between the viscid and inviscid portions of the wake was clearly defined in 9 independent photographs and measured on a photoreader machine to obtain coordinated $(x_i,y_i)$ data sets. The data were smoothed by integrating the interface over intervals of 0.5 body diameters and obtaining an average wake width for the interval. The following equations based on the work of other investigators were used in the regression analyses:

$$Y_1 = A_1 + B_1X_1{}^N \text{ (empirical)} \tag{1}$$

$$Y_2 = (A_2 + B_2X_2)^N \text{ (theoretical)} \tag{2}$$

The analyses allowed $N$ to vary over any real number. For each value of $N$, the constant $A$ and independent variable coefficient $B$ for the equation was computed. The correlation coefficient between $Y$ and $X$ was also computed to find the highest correlation coefficient. The correlation coefficient which was computed in a numerically systematic manner for all of the data was taken as a measure of the degree of fit between the data and the equation for each value of $N$. The correlation coefficient is computed as follows:

$$r = \frac{(n\Sigma X_T Y_T - \Sigma X_T \Sigma Y_T)}{\{(n\Sigma X_T{}^2 - [\Sigma X_T]^2)(n\Sigma Y_T{}^2 - [\Sigma Y_T]^2)\}^{1/2}} \tag{3}$$

where for Eq. (1)

$$Y = Y_T$$

$$X^N = X_T$$

and for Eq. (2)

$$Y^{1/N} = Y_T$$

$$X = X_T$$

Selection of the analysis giving the highest correlation coefficient for both Eqs. (1) and (2) gives the following:

$$Y = 0.0015 + 0.0221X^{1.44} \ (r = 0.720) \tag{4}$$

$$Y = (0.0123 + 0.1057X)^{2.88} (r = 0.830) \tag{5}$$

These equations are plotted in Fig. 1 with the authors' experimental data. The reason that $Y = 0$ when $X = 0$ in

Table 1 Compilation of regression equations of other investigators' data

| Investigator | Region | $M_\infty$ | Body shape | $P_\infty$ | $r$ | Regression equations |
|---|---|---|---|---|---|---|
| Fay and Goldburg | $X < 15$ | $\approx 8$ | sphere | atm | 0.56 | $Y = (0.7531 + 0.0285X)^{3.65}$ |
| Dana and Short[a] Slattery and Clay | $X < 15$ | $\approx 8$ | sphere | atm | 0.72 | $Y = (0.5328 + 0.0359X)^{2.5}$ |
| Knystautas | $X < 15$ | $\approx 5$ | sphere | atm | 0.85 | $Y = (0.4538 + 0.0186X)^{1.98}$ |
| Jenkins and Pruett | $X < 15$ | $\approx 4$ | hemisphere cylinder | atm | 0.83 | $Y = (0.1237 + 0.1057X)^{2.88}$ |
| CARDE | $100 < X < 1500$ | $\approx 6$ | sphere | atm | 0.98 | $Y = -7.9140 + 3.1957X^{0.221}$ |
| Knystautas | $30 < X < 1400$ | $\approx 5$ | sphere | atm | 0.96 | $Y = -1.0861 + 0.4903X^{0.334}$ |
| Dana and Short | $100 < X < 600$ | $\approx 5$ | sphere | atm | 0.98 | $Y = -3.7259 + 1.0254X^{0.344}$ |
| Fay and Goldburg | $20 < X < 400$ | $\approx 10$ | sphere | atm | 0.81 | $Y = 0.5135 + 0.2837\ X^{0.520}$ |

[a] Data grouped together to increase sample size.

Fig. 1 is that the origin of the coordinate system was set at the edge of the throat. In Fig. 2 the origin of the authors' data was transposed to coincide with the origin location of the other investigators.

### Discussion

The values derived for $N$ which gave the best fit as indicated by the highest correlation coefficients were 1.44 and 2.88, for the empirical and theoretical Eqs. (1) and (2), respectively. Other investigators have found values of $N$ for these equations ranging from 0.25 to about 0.67. The exponents found in this analysis were larger by a factor of about 9. These high exponents indicated that either past analyses have not sufficiently considered the near wake, or the diffusion rate is much greater in the near wake.

A search was made for near wake data which was experimentally similar to the authors' data from the standpoint of Mach number, density, pressure, and body shape. Knystautas[6] found no obvious scaling effect for projectile sizes up to factors of 12 for spheres at atmospheric pressures and velocities up to $M_\infty \approx 6$. Therefore, it was considered acceptable to compare the wakes of very short hemispheric cylinders, where $\alpha < 1°$, with the wakes of spheres under the approximate experimental conditions. On this basis, the data of other investigators were subjected to the same analysis as the authors' data.

Lees and Hromas[7] divide the wake into two functional regions with the join between the two regions forming the third region. The first region is the purely expansion controlled due to the rapid pressure drop just behind the recompression shock extending to the point where $P_w \approx 4P_\infty$. The second functional region is the thermal diffusion region which extends downstream from the point where $P_w \approx P_\infty$. In the region where $4P_\infty > P_w > P_\infty$, Lees and Hromas[7] call this the mixed expansion-diffusion region. The location in the wake at which the wake pressure is approximately four times and approximately equal to the freestream pressure is a function of $M_\infty$. The exact locations of the changes in the growth properties of the wake are not of as great concern to this analysis as the fact that the growth rate changes with $X$ and the present functions are not well fitted by a constant power dependence law for all values of $X$. Lees and Hromas[7] expected the growth rate to be greater in the expansion controlled and the mixed pressure expansion-thermal diffusion region than in the purely thermal diffusion controlled region. For the $M_\infty$ of the authors' data, the purely thermal diffusion region begins at about $X \approx 15$ (i.e., $P_\infty \approx P_\infty$). The data of other experimenters used in this analysis were separated into regions of $X < 15$ and $X > 15$. The analysis of other investigators' data also permitted $N$ to take on any value that provided the best fit (highest correlation coefficient) of $Y$ on $X$. The measure of the best fit for the data was the analysis acceptance criteria, not the fitting of the data to any one value of $N$. Since the past analyses used data predominantly in the far wake region and were obviously weighted toward thermal diffusion dependence; Eq. (1) was used by the authors for the analysis of far wake data. Table 1 shows the results of the analyses.

The analyses of all data limited to $X < 15$ resulted in values of $N > 1.0$, with correlation coefficients greater than 0.72 except for the 0.56 for Fay and Goldburg's[4] data. Analysis for the $X < 15$ data using prescribed values of $N < 1.0$ (e.g., $N = 0.33$) the correlation coefficients dropped to values in the range of 0.10 to 0.30 indicating very poor fits ($r = 1.0$ is a perfect fit). However, the data for values of $X$ in the thermal region ($P_w \approx P_\infty$) gave values of $N < 1.0$ with correlation coefficients greater than 0.95 except for Fay and Goldburg's[4] which was 0.81. Thus, for all investigators the far wake data fits the fractional power dependence much better than the near wake data. The range of values of $N$ for $X < 15$ was from 1.98 to 3.65. The range of values of $N$ for $X > 15$ was from 0.221 to 0.520 with Knystautas[6] and Dana and Short[5] approximating the 0.33 power dependence.

Experimental scatter is greater in the region of $X < 15$ as reflected by the lower correlation coefficient. However, it is not too large to detect a more rapid growth in the $X < 15$

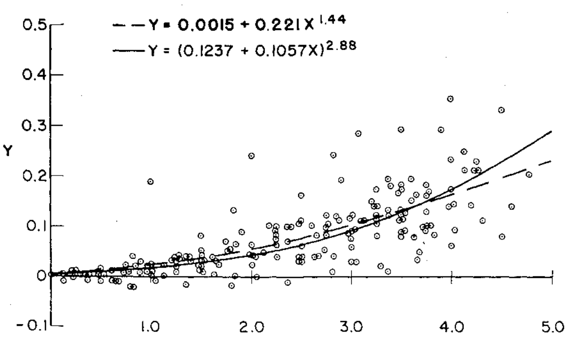


**Fig. 1 Plot of authors' experimental data and Eqs. (4) and (5).**

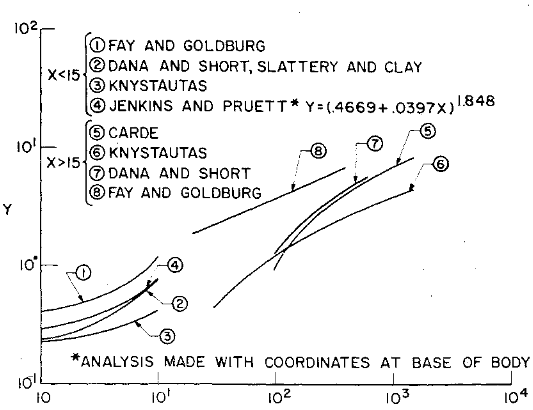


**Fig. 2 Authors' analysis of other investigators' data.**

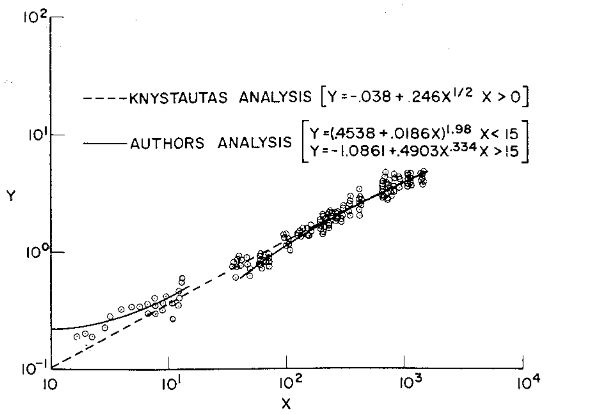


**Fig. 3 Plot of authors' analysis of Knystautas data.**

region which is appropriate for the $M_\infty$ considered in this analysis.

The data were subjected to fitting to both Eqs. (1) and (2). In cases where $X < 15$, the highest correlation coefficients were obtained with Eq. (2). In the region of $X > 15$, Eq. (1) gave the best fit reflecting its development with data weighted toward the far wake.

Figure 2 is a plot of the equations shown in Table 1. The equations representing the near wake are concave upward and the far wake are concave downward indicating that at least one inflection point exists, even though it has not been explicitly located.

Figure 3 shows a plot of Knystautas[6] reduced data along with his fit to his data. The Knystautas[6] fit shown as the dashed line was done for all values of $X$. The authors' fitting of Knystautas[6] data for $X < 15$ and $X > 15$ are shown as the solid lines. The authors' fit of Knystautas[6] data for all values of $X$ gave $N = 0.44$ which compares with the $N = 0.50$ he obtained.

### Summary

The analysis of the authors' data alone indicated that the best data fit in the pressure expansion controlled region ($P_w > 4P_\infty$) and the mixed pressure expansion-thermal diffusion region ($4P_\infty > P_w > P_\infty$) gave a value of $N > 1.0$. The same analysis of other investigators' data in the same regions also revealed values of $N > 1.0$, whereas analysis of the same data for $P_w \approx P_\infty$ revealed values of $N < 1.0$. The selection of $X \approx 15$ as the dividing point where $P_w \approx P_\infty$ is based on Lees and Hromas[7] theoretical treatment of the wake and the $M_\infty$ of the authors' data used in this analysis. The analysis shows that the rapid growth of the near wake expected by Lees and Hromas[7] does exist and is experimentally detectable. It is also apparent that analyses using data predominantly from the thermally controlled region of the far wake will result in a value of $N$ approximating the $\frac{1}{3}$ law very closely. Because the thermally controlled region is by far the larger region, analyses including all values of $X$ weighs the power dependence heavily toward the 0.33 power which is not suitable for values of $X$ where $P_w \gg P_\infty$. Equation (2) seemed to fit the data better for $X < 15$ whereas the form of Eq. (1) fit better for $X > 15$. This analysis indicates that the 0.33 power law for the wake growth is applicable only in the purely thermal region and is not applicable for all values of $X$.

### References

[1] Slattery, R. E. and Clay, W. G., "Width of the Turbulent Trail Behind a Hypervelocity Sphere," *The Physics of Fluids*, Vol. 4, 1961, pp. 1199–1201.

[2] Murphy, C. H. and Dickinson, E. R., "Growth of the Turbulent Wake behind a Supersonic Sphere," *AIAA Journal*, Vol. 1, No. 2, Feb. 1963, pp. 339–342.

[3] Wilson, L. N., "Far-Wake Behavior of Hypersonic Blunted Cones," *AIAA Journal*, Vol. 5, No. 8, Aug. 1967, pp. 1393–1396.

[4] Fay, J. A. and Goldburg, A., "The Unsteady Hypersonic Wake Behind Spheres," Paper 2676-62, Nov. 1962, ARS.

[5] Dana, T. A. and Short, W. W., "Experimental Studies of Hypersonic Turbulent Wakes," Rept. ZPH-103, 1961, General Dynamics/Convair.

[6] Knystautas, R., "The Growth of the Turbulent Inner Wake Behind a Three-Inch Diameter Sphere," TR 488, Jan. 1964, Canadian Armament Research and Development Establishment.

[7] Lees, L. and Hromas, L., "Turbulent Diffusion in the Wake of a Blunt-Nosed Body at Hypersonic Speeds," *Journal of the Aerospace Sciences*, Vol. 29, 1962, pp. 976–993.

# Viscous Effects on the Flow Coefficient for a Supersonic Nozzle

P. F. MASSIER,* L. H. BACK,† M. B. NOEL,‡ AND F. SAHELI§

*Jet Propulsion Laboratory,*
*California Institute of Technology, Pasadena, Calif.*

### Nomenclature

| | | |
|---|---|---|
| $A$ | = | area, in.$^2$ |
| $C$ | = | $[2/(\gamma+1)]^{1/(\gamma-1)}[2g\gamma/R(\gamma+1)]^{1/2}$ |
| $C_D$ | = | flow coefficient |
| $D$ | = | diameter, in. |
| $H_{t0}$ | = | stagnation enthalpy in reservoir |
| $\dot{m}$ | = | mass flow rate, lb/sec |
| $M$ | = | Mach number |
| $p$ | = | pressure, psia |
| $r$ | = | radius, in. |
| $Re_{D_{th}}$ | = | throat Reynolds number, $(\rho_e u_e D/\mu_e)_{th}$ |
| $T$ | = | temperature, °R |
| $u$ | = | velocity parallel to wall |
| $x$ | = | distance along wall |
| $y$ | = | distance normal to wall |
| $\beta$ | = | acceleration parameter |
| $\gamma$ | = | specific-heat ratio |
| $\delta$ | = | boundary-layer thickness |
| $\delta^*$ | = | displacement thickness |
| $\theta$ | = | momentum thickness |
| $\mu$ | = | viscosity |
| $\nu$ | = | kinematic viscosity |
| $\xi$ | = | transformed coordinate along wall |
| $\rho$ | = | density |

***Subscripts and superscripts***

| | | |
|---|---|---|
| $c$ | = | curvature at throat |
| $e$ | = | edge of boundary layer |
| $t$ | = | stagnation condition |
| th | = | throat condition |
| $w$ | = | wall condition |
| $(\ )^*$ | = | sonic condition |
| $1-D$ | = | one-dimensional isentropic |
| $\overline{(\ )}$ | = | mean value |

### Introduction

EXPERIMENTAL values of adiabatic flow coefficient are presented for choked flow in a supersonic nozzle which had a contour as shown in Fig. 1. Throat Reynolds numbers ranged between 650 and 350,000. Previously, there have apparently been no such measurements available for choked

Received October 30, 1969. This work represents the results of one phase of research carried out in the Propulsion Research and Advanced Concepts Section of the Jet Propulsion Laboratory, California Institute of Technology, under Contract NAS 7-100, sponsored by NASA.

* Group Supervisor.
† Member of Technical Staff.
‡ Senior Engineer.
§ Graduate Student, Colorado State University, Fort Collins, Colo.